Low-Frequency Modulation of the Longitudinal Field: Modified Rabi Envelopes

M. E. Limes, R. Glenn, R. Pankovitch, Z. Ma, M. E. Raikh, B. Saam

University of Utah, Dept. of Physics and Astronomy, 115 South 1400 East, Salt Lake City, UT 84112-0830

INTRODUCTION

The sensitivity of Rabi oscillations to low-frequency modulation (5-100 kHz) of the static longitudinal magnetic field B_0 is studied [1]. Three regimes are considered: strong modulation (compared to the driving field strength B_1, (1-10 G), fast modulation (compared to the non-modulated Rabi frequency Ω_R), and weak-resonant modulation. The experiments are straightforward to achieve in the laboratory, but can be mapped to more unconventional NMR conditions where B_1 strength is much greater than B_0 . We present experimental results that agree with predictions quantitatively, demonstrating proof-of-principle for a theory that can be applied to rotary saturation and rotational echoes [2-3], adiabatic pulsing and cross polarization [4-6], and line-narrowing techniques [7-8].

THEORY

The mapping of a weakly driven two-level system with modulation onto a strongly driven system without modulation suggests that different regimes of spin dynamics, previously known for a strongly driven system (i.e. multiphoton resonances [9-10]), can be realized under easily accessible conditions with proper choice of modulation frequency and amplitude. This mapping is obtained by relating the equation governing the rotating-wave approximation (RWA) $|{+1/2}\rangle$ amplitude $D_{+\frac{1}{2}}$ during modulation of the longitudinal field,

$$\ddot{D}_{+\frac{1}{2}} + \left[\frac{(\delta+\varepsilon_m\cos\omega_m t)^2+\Omega_R^2}{4} - i\frac{\varepsilon_m\omega_m\sin\omega_m t}{2}\right] D_{+\frac{1}{2}} = 0$$

to a non-modulated, non-RWA equation. Here, δ is the detuning of the B_1 excitation field from resonance, ε_m is the Larmor frequency associated with the modulation field, ω_m is the frequency of the modulation field, and Ω_R is the non-modulated, on-resonance Rabi frequency. This equation is solved analytically for three limiting cases: $\omega_m \gg \Omega_R$, $\varepsilon_m \gg \Omega_R \gg \omega_m$, and $\omega_m \approx \Omega_R$; $\varepsilon_m \ll \Omega_R$.

METHOD

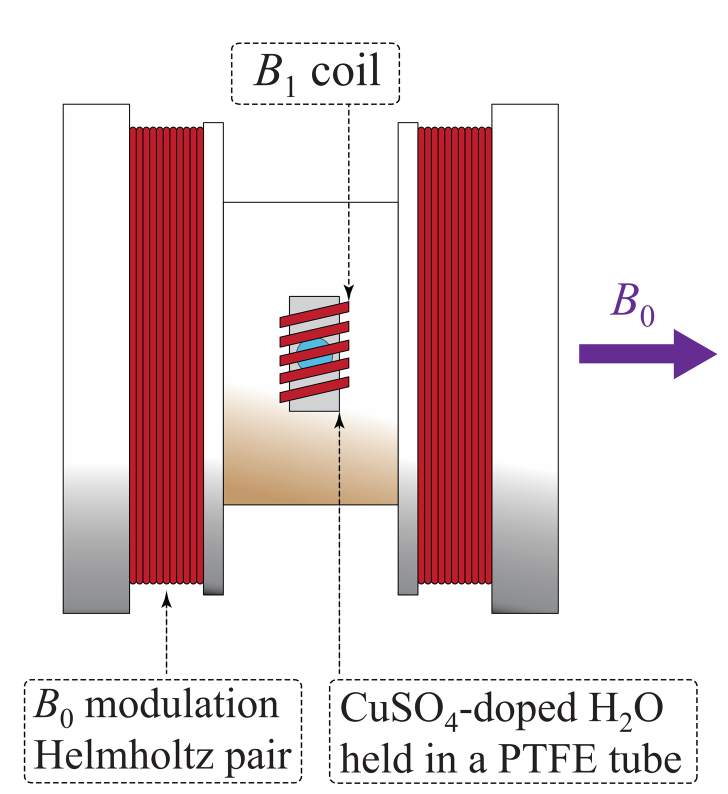

Fig. 1 A schematic and picture of the NMR probe used in the expeiments. A traditional NMR coil (B1) is accompanied by a B0 modulation Helmholtz pair that is coaxial with the B0 field.

A single-coil transmit/receive probe is series-tuned with a capacitor and 50-Ω resistor at 88.8 MHz. For B_1 homogeniety, the water sample is contained in a small PTFE tube and occupies 25% of the coil volume. B_0 modulation is provided by a 5-cm-radius Helmholtz pair (see Fig. 1) wound on a form, though an effective field can also be created by frequency modulation of B_1. The two independent transmission channels at 88.8 MHz and 0-100 kHz were controlled by a Tecmag Redstone spectrometer, which also aquired the FID. The B_1 RF pulse is amplified by a 2000W amplifier, which allowed the coherent nutation of the spins through many Rabi-oscillation periods. The B_0-modulation pulse is amplified by a DC-50 kHz gradient amplifier.

RESULTS

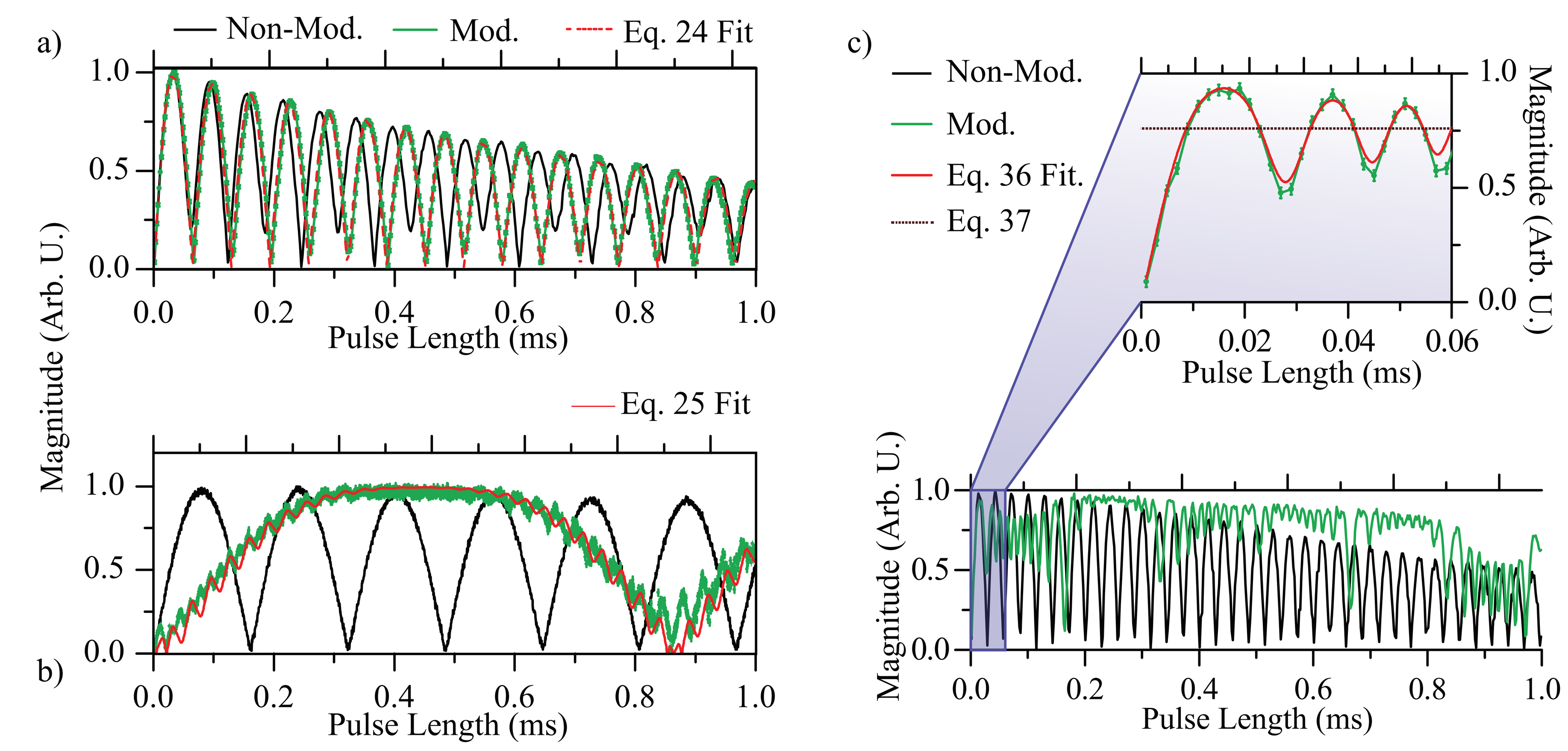

Fig. 2 (a) Fast modulation demonstrates a slowing of the Rabi frequency. (b) The fast-strong modulation regime also shows a slowing of the Rabi frequency, but also requires additional corrections to the predicted form, which is seen experimentally. (c) The effect of strong-slow modulation on Rabi oscillations is shown. This regime can be mapped to a strongly driven, non-modulated system.

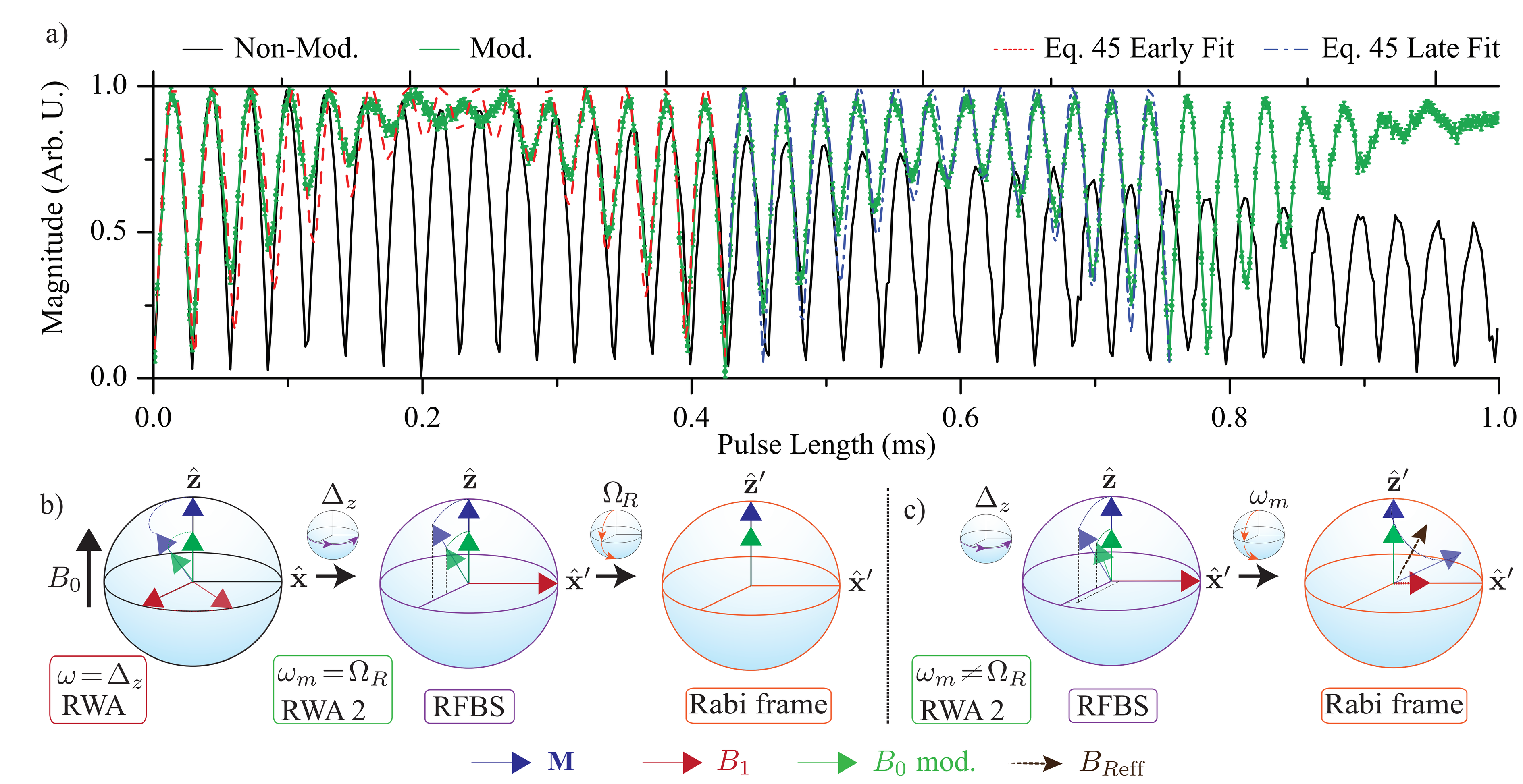

Fig. 3 (a) Shown are the results of a weak-resonant modulation and its effect on the Rabi envelope. (b) This regime lends itself to a convenient doubly rotating-frame Bloch sphere (RFBS) picture, the Rabi frame.

DISCUSSION

Fig. 2 and 3 show the results from all three regimes. Fig. 2 (a) shows fast-modulation data that results from a time-average decrease of the component of the magnetization subject to a torque generated by B_1 ; this leads to an effective Rabi frequency $\Omega_R J_0(\varepsilon_m/\omega_m)$, where J_0 is a zeroth-order Bessel function. Fig. 2 (b) shows fast-strong modulation data, where the slowing-down effect of the Rabi oscillations becomes more pronounced. Higher-order corrections manifest in the quickly oscillating components riding on top of the slow beat.

Fig. 2 (c) shows early time strong-modulation data fit to parabolic-cylinder functions. The theory also predicts the non-trivial behavior seen with periodicity $\pi/\omega_m = 0.166$ ms. Fig. 3 (a) shows weak-resonant data, where beats are observed in the Rabi oscillations. A parameter $\kappa = 2(\omega_m - \Omega_R)/\varepsilon_m$ determines the depth of the modulation; maximum modulation is for $\kappa = 1$. This maximum modulation is also understood by the Rabi frame picture developed in Fig. 3(b), where a second frame rotating at ω_m is used.

REFERENCES

[1] R. Glenn, et.al, Arxiv preprint arXiv:1212.5957.
[2] A. G. Redfield, Phys. Rev. 98, 1787 (1955).
[3] T. Gullion, Chem. Phys. Lett. 246, 325 (1995).
[4] A. Pines, M. G. Gibby, J. S. Waugh, J. Chem. Phys. 59, 569 (1973).
[5] S. Hediger, B. H. Meier, R. R. Ernst, Chem. Phys. Lett. 240, (1995).
[6] M. Garwood and L. DelaBarre, J. Magn. Reson. 153, 155 (2001).
[7] H. Kessemeier and W.-K. Rhim, Phys. Rev. B 5, 671 (1972).
[8] H. Hatanaka and N. Tabuchi, J. Magn. Reson. 155, 119 (2002).
[9] Y. Prior, J. A. Kash, and E. L. Hahn, Phys. Rev. A 18, 2603 (1978).
[10] Y. Zur, M. H. Levitt, S. Vega, J. Chem. Phys. 78, 5293 (1983).

SUPPORT: